Pharmaceutical Research, Vol. 25, No. 7, July 2008 (© 2007)
DOI: 10.1007/s11095-007-9514-y

Research Paper

Solid Lipid Nanoparticles as Delivery Systems for Bromocriptine

Elisabetta Esposito,[1,5,6] Martina Fantin,[2] Matteo Marti,[2] Markus Drechsler,[3] Lydia Paccamiccio,[4] Paolo Mariani,[4] Elisa Sivieri,[1] Francesco Lain,[1] Enea Menegatti,[1] Michele Morari,[2] and Rita Cortesi[1]

Received June 19, 2007; accepted December 3, 2007; published online January 3, 2008

Purpose. The present investigation describes a formulative study for the development of innovative drug delivery systems for bromocriptine.
Methods. Solid lipid nanoparticles (SLN) based on different lipidic components have been produced and characterized. Morphology and dimensional distribution have been investigated by electron microscopy and Photon Correlation Spectroscopy. The antiparkinsonian activities of free bromocriptine and bromocriptine encapsulated in nanostructured lipid carriers were evaluated in 6-hydroxydopamine hemilesioned rats, a model of Parkinson's disease.
Results. Tristearin/tricaprin mixture resulted in nanostructured lipid carriers with stable mean diameter up to 6 months from production. Bromocriptine was encapsulated with high entrapment efficiency in all of the SLN samples, particularly in the case of tristearin/tricaprin mixture. Bromocriptine encapsulation did not change nanoparticle dimensions. *In vitro* release kinetics based on a dialysis method demonstrated that bromocriptine was released in a prolonged fashion for 48 h. Tristearin/tricaprin nanoparticles better controlled bromocriptine release. Both free and encapsulated bromocriptine reduced the time spent on the blocks (i.e. attenuated akinesia) in the bar test, although the action of encapsulated bromocriptine was more rapid in onset and prolonged.
Conclusions. It can be concluded that nanostructured lipid carriers encapsulation may represent an effective strategy to prolong the half-life of bromocriptine.

KEY WORDS: bar test; bromocriptine (BK); cryo transmission electron microscopy; nanostructured lipid carrier (NLC); photon correlation spectroscopy (PCS); solid lipid nanoparticles (SLN).

INTRODUCTION

Nanoparticles based on solid lipids (SLN), e.g., triglycerides, have been proposed as novel drug carrier systems (1,2). SLN join the advantages of colloidal lipid emulsions with those of solid matrix particles (3). Their matrix should be able to protect labile agents from degradation and to modulate drug release profiles (4). Such lipid dispersions can be obtained by emulsification of the molten matrix lipid and subsequent recrystallization of the dispersed phase. This preparation technique makes it possible to use compositions which are exclusively based on physiological compounds, thus avoiding toxicity problems often associated with the administration of polymeric nanoparticles (5). Due to the lipophilic nature of their matrix, solid triglyceride nanoparticles are considered particularly useful for the administration of lipophilic drugs (6). The small size of triglyceride nanoparticles may allow their parenteral administration. Since they immobilize drugs more strongly than emulsions, they could serve as sustained release systems and valuable carriers for drug targeting (7). Moreover SLN can be employed to increase the specificity towards cells or tissues, to improve the bioavailability of drugs by increasing their diffusion through biological membranes and/or to protect them against enzyme inactivation (8).

The pharmacological treatment of central nervous system diseases, such as brain tumors, neurological and psychiatric disorders, is often confined by the inability of potent drugs to pass the blood brain barrier (BBB) (9–11). BBB significantly restricts water-soluble, charged and high molecular weight therapeutics to the vascular space while allowing brain parenchyma penetration of small and/or lipophilic molecules. Multiple strategies have been employed to circumvent the BBB. An emerging approach is the use of nanoparticles (12–14), which allow brain penetration to non-transportable drugs by masking their physico-chemical characteristics.

Parkinson's disease (PD) is a progressive neurodegenerative disorder characterized by a triad of motor symptoms, namely akinesia/bradykinesia, rigidity and tremor. Loss of midbrain dopamine (DA) neurons located in the *substantia*

[1] Department of Pharmaceutical Sciences, University of Ferrara, 44100 Ferrara, Italy.
[2] Department of Experimental and Clinical Medicine, Section of Pharmacology, and Istituto Nazionale di Neuroscienze, University of Ferrara, 44100 Ferrara, Italy.
[3] Macromolecular Chemistry II, University of Bayreuth, Bayreuth, Germany.
[4] Department of Science Applied to Complex Systems and CNISM, Università Politecnica delle Marche, Ancona, Italy.
[5] Dipartimento di Scienze Farmaceutiche, Via Fossato di Mortara, 19, 44100 Ferrara, Italy.
[6] To whom correspondence should be addressed. (e-mail: ese@unife.it)

nigra and subsequent dopaminergic deficit in projection areas, such as the *striatum*, underlies motor symptoms of PD (15). Drugs aimed at the reduction of the dopaminergic deficit (L-DOPA, monoamine oxidase B and catecol-*O*-methyltransferase inhibitors, dopamine agonists) remain the mainstay of symptomatic therapy of PD (16). However, development of side-effects, such as motor fluctuations and dyskinesia, limits drug effectiveness during the course of treatment (17). These side-effects, in particular dyskinesia, are thought to be due to pulsatile DA receptor stimulation which strictly reflects plasmatic L-DOPA concentrations during advanced stages of the disease (17,18). Bromocriptine (BK), the first DA agonist to be marketed more that 30 years ago, possesses slow onset of action (1–2 h) and prolonged half-life (3–5 h) (19), which probably explains the lower dyskinesiogenic potential compared to L-DOPA (20). Indeed, stabilizing plasmatic L-DOPA concentrations or using longer-acting DA agonists reduces dyskinesia (17,18).

In this respect, SLN encapsulation may represent a novel strategy to obtain stable plasma levels and increase drug half-life. To prove this hypothesis, SLN have been produced and characterized. The influence of different experimental protocols and lipidic composition on nanoparticle morphology, dimensional distribution and inner structure has been investigated. *In vitro* release kinetics of BK from SLN have also been evaluated by means of a dialysis method. Finally, the symptomatic effect of the most appropriate BK formulation has been evaluated by comparing the effects of free and SLN-encapsulated BK in the best characterized model of PD, i.e. the 6-hydroxydopamine (6-OHDA) hemilesioned (hemiparkinsonian) rat (21).

MATERIALS AND METHODS

Materials

Lutrol F 68, oxirane, methyl- polymer with oxirane (75:30; poloxamer 188) was a gift of BASF ChemTrade GmbH (Burgbernheim, Germany). Tristearin, stearic triglyceride (tristearin) was provided by Fluka (Buchs, Switzerland). Miglyol 812, caprylic/capric triglycerides (tricaprin) was purchased from Eigenmann & Veronelli (Rho, Milano, Italy). Mivaplex 600, stearic monoglyceride (monostearin) was kind gift of Eastman Ch. Company (USA). Compritol 888 ATO is a mixture of approximately 15% mono-, 50% di- and 35% triglycerides of behenic acid (C_{22}; tribehenin); it was provided by Gattefossé (Saint Priest, France). Bromocriptine mesylate (2-Bromo-α-ergocriptine methansulfonate salt; BK) was obtained from Sigma (Steinheim, Germany). Amphetamine and 6-OHDA were purchased from Sigma Chemical Company (St Louis, MO, USA).

Preparation of SLN

SLN were alternatively prepared by stirring, followed by homogenization or ultrasonication. Briefly, 1 g of lipidic mixture was melted at 75°C. The lipidic mixture concentration ranged from 3 to 10% *w*/*w* (with respect to the total weight of dispersions) and was alternatively constituted of pure tribehenin, pure tristearin, pure monostearin, tristearin/monostearin 2:1 *w*/*w*, tristearin/tricaprin 2:1 or 3:1 *w*/*w*, tribehenin/tricaprin 2:1 or 3:1 *w*/*w*. The fused lipid phase was dispersed in 19 ml of an aqueous poloxamer 188 solution (2.5% *w*/*w*) at 13,500 rpm, 75°C for 1 min, using a high-speed stirrer (Ultra Turrax T25, IKA-Werke GmbH & Co. KG, Staufen, Germany). The obtained emulsion was alternatively subjected to homogenization at 16000 r.p.m. (three cycles of 30 s) or to ultrasonication (Microson ™, Ultrasonic cell Disruptor) at 6.75 kHz for 15 min and then cooled down to room temperature by placing it in a water bath at 22°C. SLN dispersions were stored at room temperature.

In the case of BK-containing dispersions, 5 mg of the drug (0.025% *w*/*w* with respect to the total dispersions, 0.5% *w*/*w* with respect to the lipid phase) were added to the molten lipidic mixture and dissolved before adding to the aqueous solution.

Physical Characterization of SLN

Cryo-Transmission Electron Microscopy (Cryo-TEM)

Samples were vitrified as described in a previous study by Esposito *et al.* (22). The vitrified specimen was transferred to a Zeiss EM922 transmission electron microscope for imaging using a cryoholder (CT3500, Gatan). The temperature of the sample was kept below −175°C throughout the examination. Specimens were examined with doses of about 1,000–2,000 e/nm^2 at 200 kV. Images were recorded digitally by a CCD camera (Ultrascan 1000, Gatan) and processed using an image processing system (GMS 1.5 software, Gatan).

Photon Correlation Spectroscopy (PCS)

Submicron particle size analysis was performed using a Zetasizer 3000 PCS (Malvern Instr., Malvern, UK) equipped with a 5 mW helium neon laser with a wavelength output of 633 nm. Glassware was cleaned of dust by washing with detergent and rinsing twice with water for injections. Measurements were made at 25°C at an angle of 90°. Data were interpreted using the "method of cumulants" (23,24). In the cumulants method, the logarithm of the normalized correlation function $g^{(1)}(\tau)$ is expanded as a power series in the time: $\ln\left[g^{(1)}(\tau)\right] = -K_1 t + (1/2)K_2 t^2 + \ldots..$ The coefficients *Kn* are the cumulants. K_1, the first cumulant, is equal to the average of the reciprocal relaxation time $K_1 = (\Gamma)$. The second cumulant K_2 is a measure of the dispersion of the reciprocal relaxation time around the average value. Note that if K_2 (and higher order cumulants) are 0, the first order correlation function is a single exponential. The cumulant method is simple and most commercial autocorrelators include a computer program for calculating the first few cumulants (25).

X-ray Diffraction Measurements

X-ray diffraction experiments were performed using a 3.5 kW Philips PW 1830 X-ray generator (Philips, Eindhoven, The Netherlands) equipped with a Guinier-type focusing camera (Inel, Artenay, France) operating with a bent quartz crystal monochromator (λ=0.154 nm). Diffraction patterns were recorded on an Inel CPS 120 detector (Inel, Artenay, France). Samples were held in a vacuum tight cylindrical cell provided with thin mylar windows. Diffraction data were collected at room temperature (25°C), using a Haake F3

thermostat (ThermoHaake, Karlsruhe, Germany) with an accuracy of 0.1°C.

In each experiment, a number of Bragg peaks (usually 2) were observed in the low-angle X-ray diffraction region ($2\theta > 10°$, being 2θ the scattering angle), and their spacings measured. The peak indexing was performed considering the different symmetries commonly observed in lipid phases (26). From the averaged spacing of the observed peaks, the unit cell dimension, *d*, which corresponds to the distance between the mid-plane of two opposing lipid bilayers, were finally calculated by the Bragg law. The nature of the short-range lipid conformation was derived analyzing the high-angle X-ray diffraction profiles (26). It was also observed that X-ray diffraction spectra were found to be time-independent for periods of 1–2 weeks.

Drug Content of SLN Dispersions

With the aim to quantify the total drug content (free plus bonded) after SLN production, 1 ml of dispersion was added of methanol (1:4 *v*/*v*) and stirred for 3 h in order to extract completely the BK present. Afterwards, the sample was filtered with filters of 0.45 μm and analyzed by High Performance Liquid Cromatography (HPLC).

In order to separate any present free drug from SLN, 1 ml of the dispersion was loaded on a gel filtration, Sepharose 4B column (Pharmacia, Uppsala, Sweden; 2 cm diameter, 86 cm length). The void volume of the size exclusion column being 24.7 ml.

The column was pre-equilibrated and eluted with a solution of isotonic Palitzsch buffer (IPB; 5 mM $Na_2B_4O_7$, 180 mM H_3BO_3, 18 mM NaCl) pH 7.4, at a flow of 0.8 ml/min. The void volume peak fractions containing SLN were collected and extracted in methanol (1:4 *v*/*v*) and then magnetically stirred for 5 min. Afterwards, samples were filtered with filters of 0.45 μm and quantified for BK encapsulation efficiency by HPLC (see below).

In Vitro Release Kinetics of Bromocriptine from SLN

In vitro release tests were carried out with the dialysis method. Typically, 5 ml of SLN were placed into a dialysis tube (10 cm; molecular weight cut off 10,000–12,000; Medi Cell International, UK), then placed into 100 ml of citrate buffer (50 mM, pH 3.5) and ethanol (50:50, *v*/*v*) and shaken in a horizontal shaker (MS1, Minishaker, IKA, Germany) at 175 rpm at 37°C. At regular time intervals, 400 μl samples of receiving buffer were withdrawn and refilled again with fresh medium. Afterwards, samples were diluted with methanol in a 1:1 *v*/*v* ratio. The amount of drug released was determined by HPLC (using the analytical method described below).

HPLC Procedure

The HPLC determinations were performed using a HPLC system consisting of a two plungers alternative pump (Jasco, Japan), a variable wavelength UV-detector, operating at 305 nm and a Rheodyne Inc. injection valve model 7125 with a 50 μl loop.

Samples were chromatographed on a stainless steel C-18 reverse-phase column (15×0.46 cm) packed with 5 μm particles (Hypersil BDS, Alltech, USA).

Elution was conducted with a mobile phase constituted of ammonium formate (pH 3, 0.1M) and acetonitrile 55:45 *v*/*v* at a flow rate of 0.8 ml/min. The retention time for BK was 5.8 min.

The analytical validation of the HPLC method for the determination of BK was performed. The linearity, precision and repeatability values of the HPLC method were calculated and evaluated. Excellent linearity was obtained for BK between concentrations of 1.25 and 100 μg/ml in mobile phase and with $R^2=0.9997$.

The repeatability of the method was checked by the analysis of 6 replicate injections of BK in mobile phase using 3 different concentrations, namely 100, 10 and 1.25 μg/ml. These analyses were repeated throughout 3 days. The repeatability of the method was expressed as the relative standard deviation (coefficient of variation; RSD) of measured concentrations. RSD values were less than 1%.

The limit of detection-limit of quantification (LOD–LOQ) values of the HPLC method were also calculated and evaluated. LOD was estimated at a signal-to-noise ratio (S/N) of 3. LOQ was estimated at an S/N of 10. LOD and LOQ values were experimentally verified by 6 injections of BK at the LOD and LOQ concentrations. LOQ values of BK in methanol was found to be 73.5 ng/ml while LOD values was 0.22 μg /ml.

In Vitro Tests

Male Sprague–Dawley rats were kept under regular lighting conditions (12 h light/dark cycle) and given food and water *ad libitum*. The experimental protocols performed in the present study were approved by the Italian Ministero della Sanità (licence n° 111/94-B) and by Ethical Committee of the University of Ferrara. Adequate measures were taken to minimize animal pain and discomfort and to limit the number of animals employed in the study.

6-Hydroxydopamine Lesion

Unilateral lesion of dopaminergic neurons was induced in isoflurane-anaesthetised male Sprague-Dawley rats (150 g; Harlan Italy; S. Pietro al Natisone, Italy) as previously described (27). Eight micrograms of 6-hydroxydopamine (6-OHDA; dissolved in 4 μl of saline containing 0.2% ascorbic acid) were stereotaxically injected according to the following coordinates from bregma: AP=−4.4 mm, ML=−1.2 mm, VD=−7.8 mm below dura (28). In order to select the rats which had been successfully lesioned the rotational model was employed (29). Two weeks after 6-OHDA injection, rats were tested for denervation with a test dose of amphetamine (5 mg/kg i.p., dissolved in saline). Rats showing a turning behaviour >7 turns/min in a direction ipsilateral to the lesion were enrolled in the study. Experiments were usually performed 6–8 weeks after lesion. Marked (>95%) reduction in striatal DA levels and loss of tyrosine hydroxylase positive DA terminals (30) have been detected at this stage.

Behavioural Studies in Hemiparkinsonian Rats

The 6-OHDA hemilesioned rat is a well-established model of experimental parkinsonism (21), in which hypokinetic motor disturbance primarily affects the side of the body contralateral to the denervated hemisphere (i.e. the toxin

injection side). Akinesia was evaluated in hemiparkinsonian rats by the "bar test" (31), which measures the ability of the rat to respond to an externally imposed static posture. This is a valuable test for measurement of catalepsy (31) and has been validated for assessing akinesia under parkinsonian conditions (27,30). Each rat was placed gently on a table and the contralateral and ipsilateral forepaws were placed alternatively on blocks of increasing heights (3, 6 and 9 cm). The immobility time (in sec) of each paw on the blocks was recorded (cut-off time of 20 s). Rats were trained on the bar until their motor performance was reproducible. Akinesia was calculated as total time spent on the blocks (in seconds) by the contralateral (i.e. parkinsonian) forepaw or by the contralateral plus the ipsilateral forepaw (as an index of overall akinesia), and expressed as percent of pre-treatment values. Saline, free BK (3 mg/kg), empty tristearin/tricaprin SLN or BK containing tristearin/tricaprin SLN (3 mg/kg) were given intraperitoneally (i.p.) in a volume of 500 µl to 21 6-OHDA hemilesioned rats.

Statistical Analysis

Statistical analysis was performed on percent data (GraphPad Prism software, San Diego, CA, USA) by two-way analysis of variance (ANOVA) with repeated measures followed by the Newman-Keuls test for multiple comparisons. P values <0.01 were considered to be statistically significant.

RESULTS

Production and Characterization of SLN

SLN were obtained from different lipid mixtures and concentrations, using two alternative methods based on homogenization and ultrasonication. Lipid concentration was found to affect the physical aspect of the dispersion: the higher the lipid content, the greater the consistence of the dispersions, passing from fluid (lipidic mixture 3, 4, 5% *w*/*w* with respect to the total weight of the dispersions) to semi-fluid (6–7% *w*/*w*) to semisolid (10% *w*/*w*). The use of pure monostearin did not lead to nanoparticle formation. The mixture tribehenin/tricaprin (2:1) resulted in unstable nanoparticle dispersions, with mean diameters dramatically increasing by time (data not shown). On the other hand, the use of tristearin, pure or in mixture with monostearin or tricaprin, and the use of pure behenin led to results depending on the procedure employed.

Table I. Mean Diameters of SLN* Based on Different Lipid Compositions as Determined by PCS

		Lipid Composition			
Time	Parameter	Tristearin	Tristearin/Monostearin (2:1)	Tristearin/Tricaprin (2:1)	Tribehenin
0 days	ZAverage[a] (nm)	217 [b]	163 [b]	196 [b]	180 [b]
		222 BK [c]	215 BK [c]	195 BK [c]	300 BK [c]
	P.I.[d]	0.20 [b]	0.44 [b]	0.24 [b]	0.32 [b]
		0.30 BK [c]	0.67 BK [c]	0.22 BK [c]	0.69 BK [c]
30 days	ZAverage[a] (nm)	228 [b]	171 [b]	195 [b]	189 [b]
		227 BK [c]	300 BK[c]	200 BK [c]	385 BK [c]
	P.I.[d]	0.32 [b]	0.44 [b]	0.22 [b]	0.41 [b]
		0.35 BK [c]	0.28 BK [c]	0.31 BK [c]	0.6 BK [c]
60 days	ZAverage[a] (nm)	223 [b]	171 [b]	195 [b]	193 [b]
		225 BK [c]	428 BK [c]	201 BK [c]	n.d.[e] BK [c]
	P.I.[d]	0.32 [b]	0.50 [b]	0.24 [b]	0.34 [b]
		0.33 BK [c]	1.00 BK [c]	0.21 B [c]	1.00 BK [c]
90 days	ZAverage[a] (nm)	224 [b]	178 [b]	200 [b]	225 [b]
		226 BK [c]	478 BK [c]	200 BK [c]	n.d.[e] BK [c]
	P.I.[d]	0.35 [b]	0.46 [b]	0.24 [b]	0.35 [b]
		0.34 BK [c]	1.00 BK [c]	0.23 BK [c]	1.00 BK [c]
120 days	ZAverage[a] (nm)	228 [b]	163 [b]	203 [b]	186 [b]
		227 BK [c]	502 BK [c]	203 BK [c]	n.d.[e] BK [c]
	P.I..[d]	0.30 [b]	0.45 [b]	0.25 [b]	0.35 [b]
		0.30 BK [c]	0.95 BK [c]	0.24 BK [c]	1.00 BK [c]
150 days	ZAverage[a] (nm)	225 [b]	166 [b]	204 [b]	344 [b]
		227 BK [c]	533 BK [c]	203 BK [c]	n.d.[e] BK [c]
	P.I.[d]	0.35 [b]	0.43 [b]	0.28 [b]	0.65 [b]
		0.34 BK [c]	1.00 BK [c]	0.28 BK [c]	1.00 BK [c]
180 days	ZAverage[a] (nm)	215 [b]	159 [b]	200 [b]	n.d.[e]
		228 BK [c]	559 BK [c]	203 BK [c]	n.d.[e] BK [c]
	P.I.[d]	0.37 [b]	0.43 [b]	0.21[b]	n.d.[e]
		0.38 BK [c]	1.00 BK [c]	0.25 BK [c]	1.00 BK[c]

PCS data are means of five determinations on different batches of the same type of dispersion, SD was always comprised between ±5%
[*] SLN were obtained by sonication method
[a] Determined by PCS
[b] SLN produced in the absence of Bromocriptine
[c] SLN produced in the presence of Bromocriptine
[d] Polidispersity Index
[e] not determinable by the instrument.

In particular, the homogenization method resulted in the production of unstable dispersions with broad dimensional distributions. Conversely the use of sonication enabled us to obtain stable and homogenous dispersions, free from aggregates.

Table I summarizes the results obtained by a PCS study on SLN obtained by sonication using different lipid phases. Pure tristearin led to the larger mean diameter (216.8 nm) and a bimodal distribution. The tristearin/monostearin mixture resulted in a smaller mean diameter (154.3 nm) but in a broad distribution (0.43 Polydispersity Index, P.I.); the best results were obtained with tristearin/ tricaprin (mean diameter 197.5, monomodal distribution, P.I. 0.22). SLN dispersions of tristearin, tristearin/monostearin and tristearin/tricaprin maintained their dimensions almost unchanged for more than 6 months. As summarized in Table I, BK encapsulation in SLN led to an increase in mean diameter after 6 months, except in the case of tristearin/tricaprin SLN. Mean diameters of tristearin/monostearin SLN doubled after 2 months from production, while, after the same period, behenin SLN dramatically increased to undetectable dimensions.

It has to be considered that SLN with BK could have a bigger median diameter than the filter pores and thus influence the quantitative analysis of drug content of SLN dispersions. In this view, the final fraction of SLN was evaluated by difference with respect to the weight of the larger particles separated from dispersion by filtration. Percentage of two particles population was referred to the weight of disperse phase before production. Moreover the loss of disperse phase on the vessel before dispersion into poloxamer solution was evaluated. In particular it was found the highest lost was on the vessel (around 4% *w*/*w* with respect to the weight of lipid phase before dispersion) whilst larger particles represented less than 1% with respect to the total weight of disperse phase. However, the acquired quantity of drug content was found consistent with that previously weighted for the SLN preparation.

Cryo-transmission electron microscopy (Cryo-TEM) analyses were conducted in order to shed light on the internal structure of the dispersed particles in SLN dispersions.

It is worth mentioning that monostearin, tristearin and tribehenin are solid lipids, while tricaprin is a liquid oil at room temperature. Therefore the use of tricaprin in mixture with solid lipids leads to the formation of solid carriers with homogenous lipid nanocompartments (nanostructured lipid carriers, NLC) rather than solid lipid nanoparticles (SLN).

Figure 1 shows cryo-TEM images of SLN dispersions constituted of Tristearin (A), Tristearin-Monostearin (2:1) (B), Tristearin-Tricaprin (2:1) (C), Tribehenin (D) and BK-containing Tristearin-Tricaprin (2:1) SLN dispersion (E). The three dimensional particles are projected in a two dimensional way. In all panels one can observe deformed hexagonal, elongated circular platelet-like crystalline particles (SLN/NLC top views) and dark, "needle" like structures edge-on viewed (SLN NLC side views). The measured thickness of nanoparticles is between ca. 5 nm and 40 nm according to the number of layers in the platelets. The exact thickness is difficult to measure because the tilt of the particles can not exactly be determined. In panel C, besides the presence of hexagonal and circular SLN top views, the "needles" respect the SLN side views are more elliptically shaped. This may be attributed to the presence of tricaprin, which is liquid at room temperature and forms caps on the surfaces of the SLNs. This is less pronounced in the presence of BK which does not further affect nanoparticles aspect (panel E).

X-ray diffraction profiles were analyzed considering separately the low-angle diffraction region, from which information on the long-range organization of the lipid structure elements can be derived, and the high-angle diffraction region, from which the nature of the short-range lipid conformation can be obtained. Data for samples from *a* to *d* are not shown.

Samples *b* and *d* show a 2 narrow Bragg peaks in the low-angle region, while a series of reflections are detected in the high-angle region. As the position of the low-angle peaks indexes in a 1-D lattice, the lamellar organization can be deduced. However, the high-angle region indicates that the order inside the lamellae is crystalline. The comparison between the two profiles indicates that the presence of BK does not modify the tristearin lattice. Samples *a* and *c* show a smaller number of Bragg reflections, both at low and at high angle. In the low-angle region, the peaks are diffuse (wide),

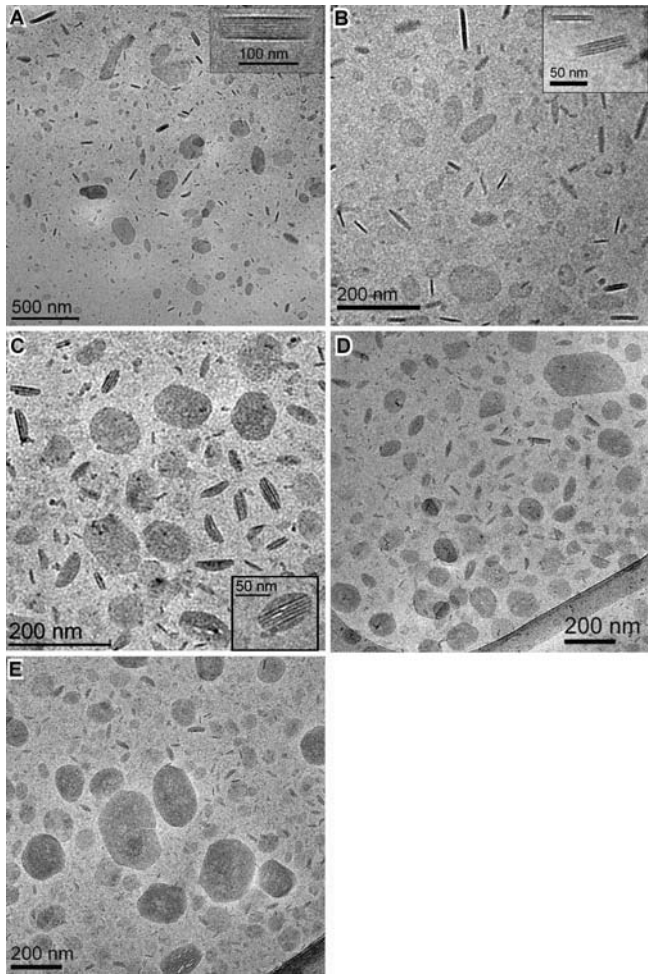

Fig. 1. Cryo-transmission electron microscopy images (cryo-TEM) of SLN dispersions constituted of tristearin (**A**), tristearin–monostearin (2:1) (**B**), tristearin–tricaprin (2:1) (**C**), tribehenin (**D**) and tristearin–tricaprin (2:1) containing bromocriptine (BK) (**E**). The insets show in more detail the shape of the SLNs *versus* NLCs. Each panel has its own scale bar.

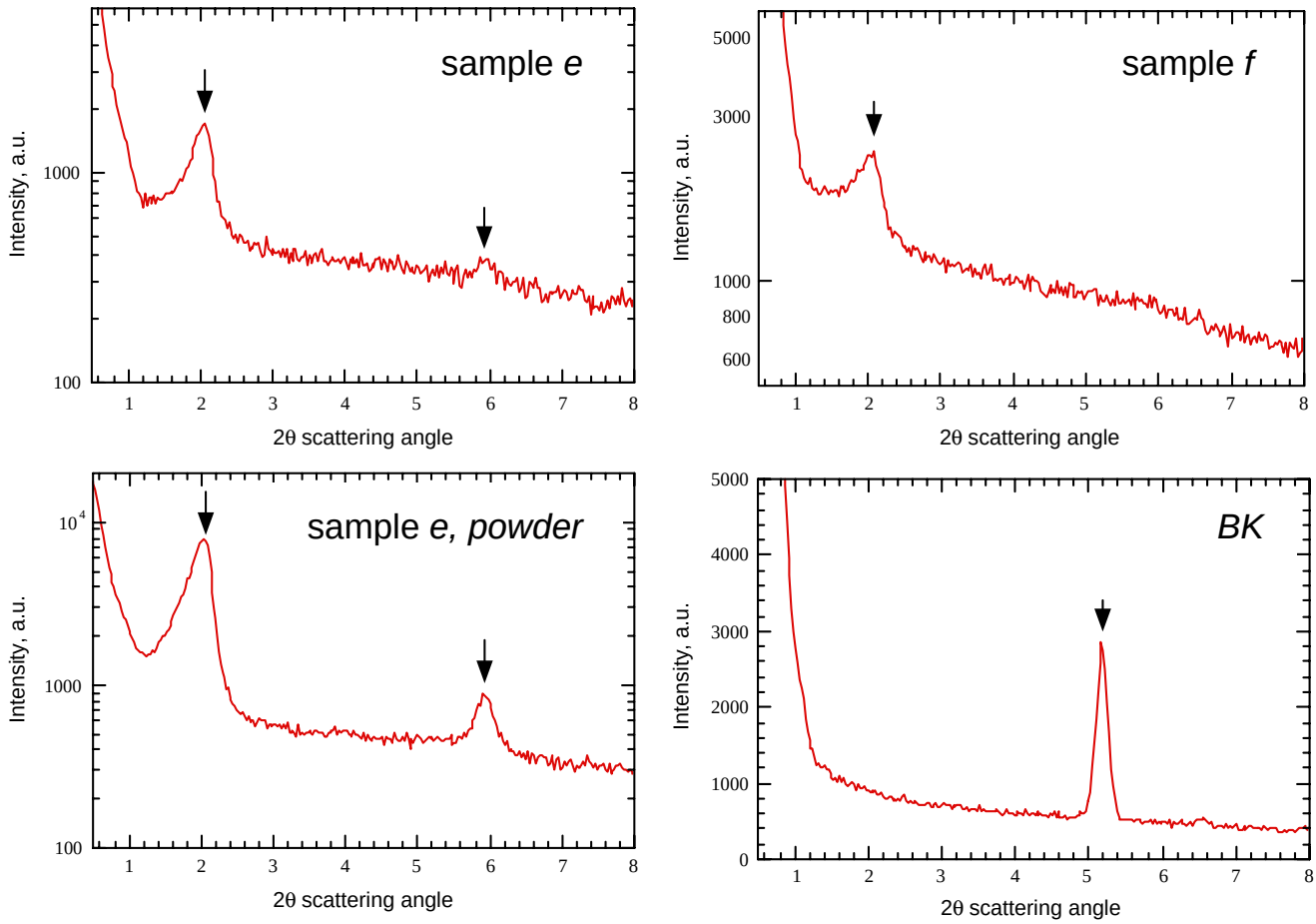

Fig. 2. Low-angle X-ray diffraction profiles obtained from tristearin–tricaprin samples with and without bromocriptine. Top frames, from left to right: SLN dispersions constituted of tristearin–tricaprin (2:1) (sample *e*), and tristearin–tricaprin (2:1) containing bromocriptine (sample *f*). As comparison, lower frames show the low angle diffraction profiles form tristearin–tricaprin (2:1) powder mixed with BK before SLN production (*left frame*) and a crystalline powder of bromocriptine (*right frame*).

and a second order (which should confirm the presence of a lamellar lattice) can hardly be detected. In the high-angle region, only a few peaks are observed, suggesting that the order of the hydrocarbon chains is scarcely periodic. In both cases, the phase is probably a gel lamellar phase.

Therefore, *a* and *c* samples show a very low degree of order, which may be due to a small extension of the crystallite or to a presence of numerous defects.

The tristearin–tricaprin system was then studied in detail, considering the effect of the addition of BK (samples *e* and *f*). The low-angle scattering profiles for the two samples are reported in Figure 2, together with the corresponding profile obtained by a crystalline powder of BK. The presence of 2 peaks and their positions indicate that the triglyceride systems form a lamellar phase, both in the presence and in absence of the drug. As reported in Table II, the addition of BK does not change the lamellar unit cell. It is interesting to observe that the peak present in the BK powder disappears when the drug is dissolved in the mixture. The high-angle data are shown in Fig. 3, together with the scattering profile obtained by

Table II. Structural Organization of SLN at Different Lipid Compositions as Derived by X-ray Diffraction Analysis

	Lipid Composition	Phase	Unit Cell	Hydrocarbon Chain Conformation
a	Tristearin/monostearin	L_G	48.2 Å	gel
b	Tristearin	L_C	45.3 Å	crystalline
c	Tribehenin	L_G	59.9 Å	gel
d	Tristearin /tricaprin (2:1) + BK powder	L_C	44.3 Å	crystalline
e	Tristearin/tricaprin	L_G	47.8 Å	gel
f	BK tristearin /tricaprin (2:1)	L_G	47.8 Å	gel

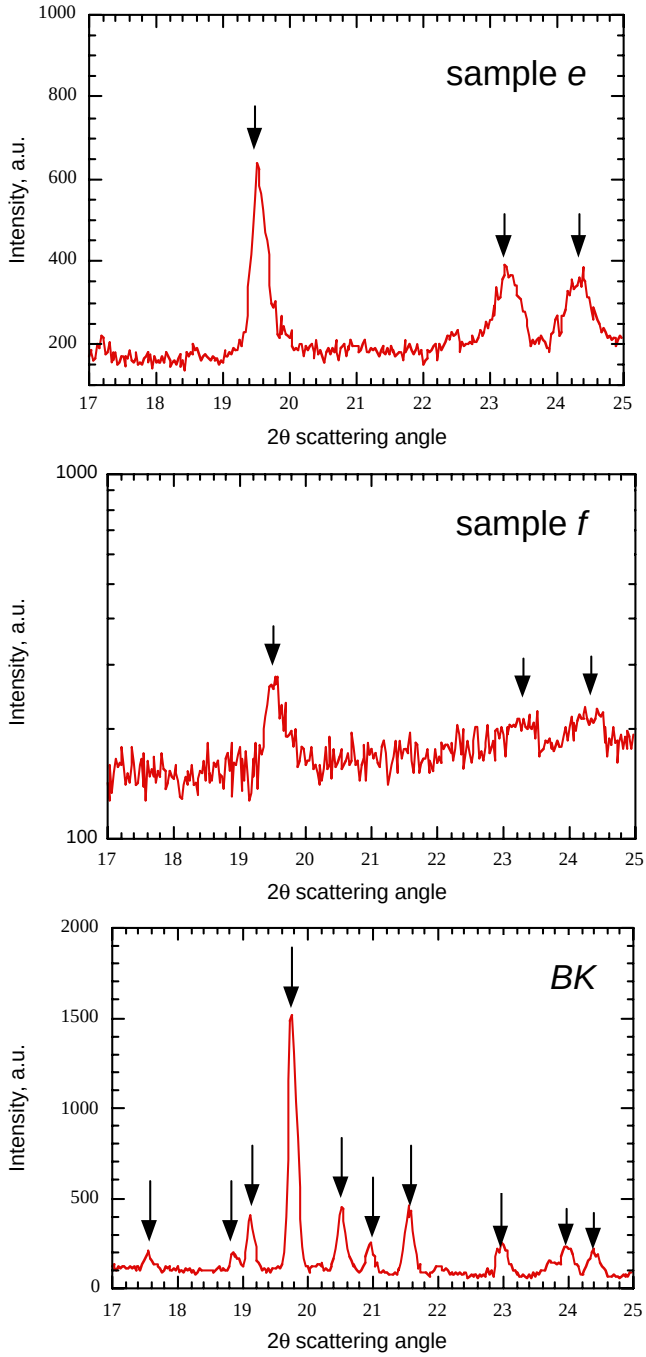

Fig. 3. High angle X-ray diffraction profiles obtained from tristearin–tricaprin samples with and without bromocriptine. From the top: SLN dispersions constituted of tristearin–tricaprin (2:1) (sample *e*), and tristearin–tricaprin (2:1) containing BK (sample *f*). As a comparison, the high angle diffraction profile observed from a crystalline powder of bromocriptine is also shown in the lower frame.

tristearin–tricaprin (2:1) powder. It can be observed that after the addition of BK the scattering profile remains unchanged, indicating that the order inside the hydrocarbon chains is still conserved. The drug is then perfectly solubilized by the triglyceride mixture.

Efficiency of BK Encapsulation in SLN

BK encapsulation yield (Table III) was similar in the case of tristearin alone, tristearin–monostearin (2:1) and tribehenin (about 75%, with respect to the total amount used for the preparation), but higher (84%) in the case of tristearin–tricaprin (2:1). Therefore it can be asserted that the homogenous lipid nanocompartments of nanostructured lipid carriers promote BK encapsulation rather than solid lipid nanoparticles.

In Vitro Release Kinetics

In order to obtain quantitative and qualitative information on drug release from the SLN, the complete release profile of SLN-encapsulated BK was determined by an *in vitro* dialysis method.

Figure 4 shows the release kinetics of free BK compared to that of BK encapsulated in SLN obtained by different lipid mixtures. Drug release was always slower for SLN-encapsulated than free BK. Moreover, the slowest release was observed for SLN produced by tristearin/tricaprin mixture, which released as much as 74% of drug content at 48 h.

In Vivo Tests

In 6-OHDA hemilesioned rats, motor impairment mainly affects the side of the body contralateral to the denervated hemisphere (i.e. the toxin injection side). Consistently, the immobility time of the ipsilateral paw (21.7±2.0 s; n=20) was lower compared to that of the contralateral one (34.2±2.0, n=20). These parameters were not changed by saline administration (data not shown). Repeated measure ANOVA on the contralateral paw (Fig. 5A) revealed main effect of treatment ($F_{13,15}$=7,99, p<0.0001), time ($F_{3,9}$=13.09, p<0.0001) and a time x treatment interaction ($F_{9,171}$=944,86, p<0.0001). Post-hoc analysis showed that both free and encapsulated BK reduced the time spent on bar (i.e. attenuated akinesia) compared to vehicle-treated animals, although the action of encapsulated BK was more rapid in onset and prolonged (Fig. 5A). Indeed, encapsulated BK was effective already 30 min after administration and its action still close to maximum 5 h after administration. Conversely, the action of free BK was slower in onset and short-lasting, since it disappeared within 5 h. A similar pattern of response was observed when the immobility time of the ipsilateral plus the contralateral paw (overall akinesia) was calculated (Fig. 5B).

DISCUSSION

The present investigation describes a formulative study for the development of innovative drug delivery systems for an old antiparkinsonian drug (i.e. the DA receptor agonist BK). SLN based on different lipidic components were produced and characterized, and their morphology and dimensional distribution investigated. BK was encapsulated with the highest entrapment efficiency in a tristearin/tricaprin mixture able to guarantee long term stability and prolonged drug release. High angle X-ray diffraction demonstrated that the presence of BK did not affect the scattering profile, indicating a maintenance of the order inside the hydrocarbon

Table III. Bromocriptine Content and Encapsulation Efficiency in SLN

Parameter	Lipid		Composition	
	Tristearin	Tristearin/Monostearin (2:1)	Tristearin/Tricaprin (2:1)	Tribehenin
Drug content (%)[a]	0.33±0.01	0.35±0.02	0.38±0.02	0.31±0.01
Encapsulation yield (%)[b]	76±0.50	74±0.62	84±0.58	76±0.35

Data are means of four independent determinations.
[a] Percentage (*w*/*w*) of BK content with respect to the lipid phase.
[b] Percentage (*w*/*w*) of encapsulated BK with respect to the total amount used for the preparation.

chains. BK was then perfectly solubilized by the tristearin/tricaprin mixture. This mixture resulted in the formation of NLC, where the presence of tricaprin created oil droplets on the surface of the SLN cores (32). As reported by other authors, drug release is controlled by the surrounding solid lipid barrier and firmly included during long time established (4,8). Accordingly, in the present investigation the slowest BK release was found in the case of tristearin/tricaprin NLC. For all these reasons of the latter formulation was selected for *in vivo* studies. These studies indicated that the antiparkinsonian action of encapsulated BK was more rapid in onset and long-lasting compared to that of free BK, suggesting that NLC encapsulation may represent a novel and effective strategy to provide stable plasmatic drug levels and prolong BK action.

The advantages of using SLN for drug delivery have been well demonstrated (1–8). Moreover, it is an interesting finding that SLN (non-stealth or stealth) appear by their nature to be capable of overcoming BBB. However the translocation mechanism of nanoparticles into the brain remains not fully understood. Olivier and colleagues (33) have suggested that nanoparticles could open the tight junctions between endothelial cells in the brain microvasculature, thus creating a paracellular pathway for nanoparticle translocation. Other authors have suggested simple passive diffusion, transport and or endocytocis (34–36). After intravenous administration colloidal systems dramatically interact with plasma proteins by the "opsonization" process. By this process, hydrophobic colloidal particles are coated with plasma components and rapidly removed from the circulation by the macrophages of the liver and the spleen, owning specific receptors for these opsonins (37–40). Only small and hydrophilic enough colloidal particles can escape from the

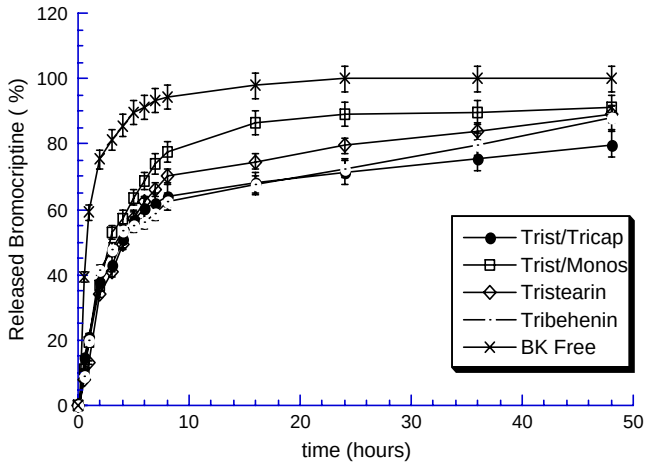

Fig. 4. *In vitro* release kinetics of bromocriptine incorporated in the indicated SLN dispersions, as determined by dialysis method. Data are means ± SEM of six independent determinations.

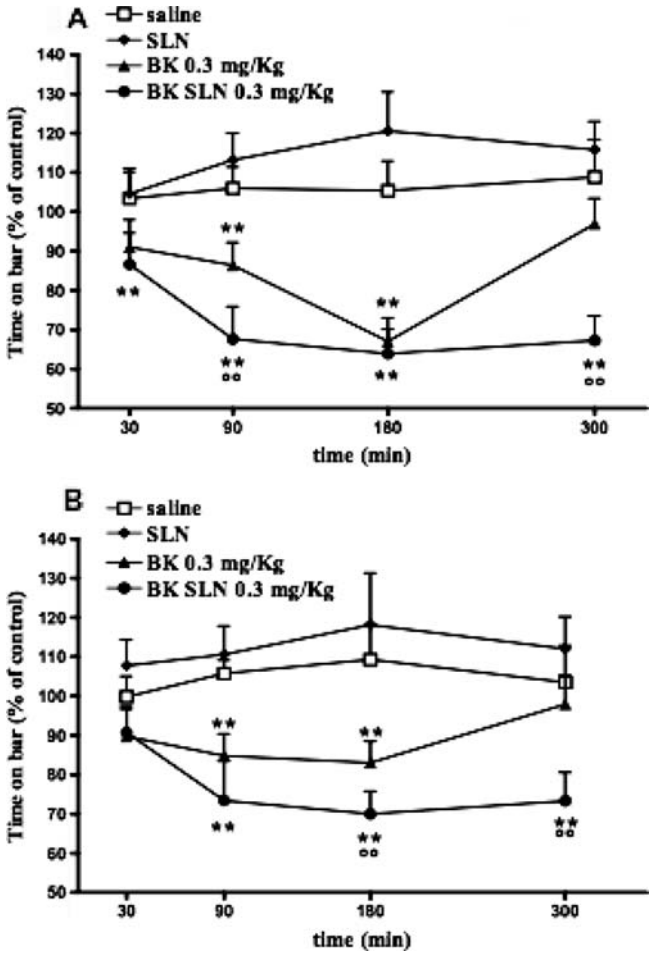

Fig. 5. Systemic injections of free bromocriptine (BK; 0.3 mg/kg, i.p.) or bromocriptine incapsulated in nanoparticles (BK SLN; 0.3 mg/kg; i.p.) attenuated akinesia in hemiparkinsonian rats. Akinesia was calculated at different time-points (30, 90, 180, 300 min from injection) as the sum of time spent on the blocks by both the contralateral and the ipsilateral forepaw (in seconds) and expressed as percent of pre-treatment values. Akinesia at the contralateral forepaw is shown in **A** whereas akinesia at the contralateral plus ipsilateral forepaw (overall akinesia) is shown in **B**. Data are means ± SEM of 13–16 determinations. $^{**}p<0.01$ different from respective control (saline or SLN)^{00} $p<0.01$ different from free BK.

opsonization process and consequently remain in the circulation for a relatively prolonged period of time.

In order to enhance the SLN distribution in the brain, some authors have proposed surface modification of SLN by Pluronic F-68, poly(ethylene glycol)- or by polysorbate 80 (40–42). The modification causes steric hindrance effect, decreasing the adsorption of opsonin to SLN in plasma. This effect retards the rapid removal of particles by the reticulo-endothelial system and enhances the transport across the endothelial cell layer and the delivery to the brain (36). As discussed before by others (42–45), SLN have unique advantages as drug carriers. In addition, it should be underlined that to the aim of this work is not important to know exactly if and where SLN pass and stay within the brain, but only that they are able to increase at the brain level the drug concentration (44) and also maintain the release for a longer period of time with respect to the corresponding free drug.

The results obtained in the present investigation demonstrated that in the case of BK containing NLC there was no need to modify nanoparticle surface in order to deliver the drug to the brain.

The 6-OHDA hemilesioned rat is the best-characterized rodent model of PD (21). Selective DA depletion of one striatum induces motor asymmetry, with the side of the body contralateral to the lesioned hemisphere being more severely affected than the ipsilateral one. This model has been widely used to screen for antiparkinsonian drugs since high doses of DA agonists or DA releasing drugs cause contralateral or ipsilateral turning, respectively, depending on the side of DA receptor stimulation. More recently, the usefulness of turning evaluation in predicting the antiparkinsonian potential of a drug has been questioned (46). Thus, behavioural tests aimed at assessing movements in a more physiological setting (i.e. without the use of a stimulating drug) have been increasingly developed. The bar test was originally developed to assess acute drug-induced catalepsy (28). Nevertheless, we recently validated it for quantification of both the akinesia induced by unilateral 6-OHDA lesioning and the motor improvement induced by L-DOPA administration (24,27). Consistent with these studies, a DA agonist such as BK was found effective in attenuating motor asymmetry at the contralateral paw, although its profile of action was dramatically modified by encapsulation in NLC. Indeed, although the maximal efficacy was not different between free and NLC-encapsulated BK, the delay of action of encapsulated BK was shorter and the duration longer lasting compared to free BK. Improvement of pharmacokinetic properties may underlie such a difference: an increased metabolic stability and/or brain penetration may explain the rapid onset of action whereas a prolonged BK release from NLC the long lasting response. It is likely that this novel drug delivery system extends BK half-life and prolongs its antiparkinsonian action. Moreover, seeing the time-course of the antiakinetic effect which remains close to maximum from 90 min onwards (up to 5 h), it may be that stable brain levels of BK are achieved during such a long period. In clinical practice, achieving a stable and long lasting response to a DA agonist appears desirable not only for reduction of frequency of administration but also to prevent development of long-term side effects such as dyskinesia. Indeed, dyskinesia is thought to arise from abnormal (pulsatile) DA receptor stimulation causing upregulation of opioid striatal precursors (priming effect; (17)). According to the notion of continuous DA receptor stimulation (18), long-acting DA agonists are less prone to prime the brain and cause dyskinesia than conventional L-DOPA formulations.

CONCLUSIONS

The encouraging results reported above suggest that NLC based on tristearin/tricaprin mixture could be proposed as innovative system to administer BK in the course of PD therapy. Other studies are required to ascertain whether this innovative drug delivery system can be used to formulate other DA agonists and L-DOPA itself. Nevertheless, this system may represent a novel strategy to achieve stable drug levels thereby increasing patient's compliance to the therapy and reducing long-term side effects.

ACKNOWLEDGEMENTS

Authors are grateful to Dr. Fabrizio Bortolotti (University of Ferrara) for HPLC technical assistance. This work was supported by Regione Emilia Romagna, Spinner Project.

REFERENCES

1. H. Bunjes, M. Drechsler, M. H. J. Koch, and K. Westesen. Incorporation of the Model Drug Ubidecarenone into Solid Lipid Nanoparticles. *Pharm. Res.* **18**:287–293 (2001).
2. K. Westesen and B. Siekmann. Biodegradable colloidal drug carrier systems based on solid lipids. In S. Benita (ed.), *Microencapsulation*, Marcel Dekker, New York, 1996, pp. 213–258.
3. K. Westesen, H. Bunjes, and M. H. J. Koch. Physicochemical characterization of lipid nanoparticles and evaluation of their drug loading capacity and sustained release potential. *J. Control Rel.* **48**:223–223 (1997).
4. R. H. Muller, K. Mader, and S. Gohla. Solid lipid nanoparticles (SLN) for controlled delivery-a review of the state of the art. *Eur. J. Pharm. Biopharm.* **50**:161–177 (2000).
5. W. Mehnert and K. Mader. Solid lipid nanoparticles: production, characterization and applications. *Adv. Drug. Deliv Rev.* **47**:165–196 (2001).
6. A. Dingler and S. H. Gohla. Production of solid lipid nanoparticles (SLN): scaling up feasibilities. *J. Microencapsul.* **19**:11–18 (2002).
7. V. Jenning, A. Lippacher, and S. H. Gohla. Medium scale production of solid lipid nanoparticles (SLN) by high pressure homogenisation. *J. Microencapsul.* **19**:1–10 (2002).
8. A. Lippacher, R. H. Muller, and K. Mader. Preparation of semisolid drug carriers for topical application based on solid lipid nanoparticles. *Int. J. Pharm.* **214**:9–12 (2001).
9. A. V. Kabanov and E. V. Batrakova. New technologies for drug delivery across the blood brain barrier. *Curr. Pharm. Des.* **10**:1355–1363 (2004).
10. J. Temsamani, J. M. Scherrmann, A. R. Rees, and M. Kaczorek. Brain drug delivery technologies: novel approaches for transporting therapeutics. PSTT. **3**:2000 (2000).
11. E. H. Lo, A. B. Singhal, V. P. Torchilin, and N. J. Abbott. Drug delivery to damaged brain. *Brain Res. Brain Res. Rev.* **38**:140–148 (2001).
12. N. Bodor and P. Buchwald. Recent advances in the brain targeting of neuropharmaceuticals by chemical delivery systems. *Ad. Drug Deliv. Rev.* **36**:229–254 (1999).
13. T. Terasaki and K. Hosoya. The blood–brain barrier efflux transporters as a detoxifying system for the brain. *Adv. Drug Deliv. Rev.* **36**:195–209 (1999).

14. E. Garcia-Garcia, K. Andrieux, S. Gilb, and P. Couvreur. Colloidal carriers and blood–brain barrier (BBB) translocation: A way to deliver drugs to the brain. *Int. J. Pharm.* **298**:274–292 (2005).
15. A. J. Hughes, S. E. Daniel, S. Blankson, and A. J. Lees. Clinicopathologic study of 100 cases of Parkinson's disease. *Arch. Neurol.* **50**:140–148 (1993).
16. O. Rascol, C. Goetz, W. Koller, W. Poewe, and C. Sampaio. Treatment interventions for parkinson's disease: an evidence based assessment. *Lancet.* **359**:1589–1598 (2002).
17. J. A. Obeso, C. W. Olanow, and J. G. Nutt. Levodopa motor complications in Parkinson's disease. *Trends Neurosci.* **23**:S2–S7 (2000).
18. J. A. Obeso, F. Grandas, M. T. Herrero, and R. Horowski. The role of pulsatile *versus* continuous dopamine receptor stimulation for functional recovery in Parkinson's disease. *Eur. J. Neurosci.* **6**:889–897 (1994).
19. T. Kvermo, S. Hartter, and E. Burger. A review of the receptor-binding and pharmacokinetic properties of dopamine agonists. *Clin. Ther.* **28**:1065–1078 (2006).
20. R. K. B. Pearce, T. Banerji, P. Jenner, and C. D. Marsden. De novo administration of ropinirole and bromocriptine induces less dyskinesia than L-DOPA in the MPTP-treated marmoset. *Mov. Disord.* **13**:234–241 (1998).
21. R. K. W. Schwarting and J. P. Huston. The unilateral 6-hydroxydopamine lesion model in behavioral brain research. Analysis of functional deficits, recovery and treatments. *Prog. Neurobiol.* **50**:275–331 (1996).
22. E. Esposito, N. Eblovi, S. Rasi, M. Drechsler, G. M. Di Gregorio, E. Menegatti, and R. Cortesi. Lipid based supramolecular systems for topical application: a preformulatory study. AAPS PharmSci. **5**:4 Article 30 (2003).
23. D. E. Koppel. Analysis of macromolecular polydispersity in intensity correlation spectroscopy: The method of cumulants *J. Chem. Phys.* **57**:4814–4820 (1972).
24. http://en.wikipedia.org/wiki/Dynamic_light_scattering.
25. R. Pecora. Dynamic Light Scattering Measurement of Nanometer Particles in Liquids J. *Nanoparticle Res.* **2**:123–131 (2000).
26. P. Mariani, V. Luzzati, and H. Delacroix. Cubic phases of lipid-containing systems. Structure analysis and biological implications. *J. Mol. Biol.* **204**:165–189 (1988).
27. M. Marti, F. Mela, M. Fantin, S. Zucchini, J. M. Brown, J. Witta, M. DiBenedetto, B. Buzas, R. K. Reinscheid, S. Salvadori, R. Guerrini, P. Romualdi, S. Candeletti, M. Simonato, B. M. Cox, and M. Morari. Blockade of nociceptin/orphanin FQ transmission attenuates symptoms and neurodegeneration associated with Parkinson's disease. *J. Neurosci.* **95**:9591–9601 (2005).
28. G. Paxinos and C. Watson. The rat brain in stereotaxic coordinates. Ed. Academic, Sydney (1982).
29. U. Ungerstedt and G. W. Arbuthnott. Quantitative recording of rotational behaviour in rats after 6-hydroxydopamine lesions of the nigrostriatal dopamine system. *Brain Res.* **24**:485–493 (1970).
30. M. Marti, C. Trapella, R. Viaro, and M. Morari. The nociceptin/orphanin FQ receptor antagonist J-113397 and L-DOPA additively attenuate experimental parkinsonism through overinhibition of the nigrothalamic pathway. *J. Neurosci.* **27**:1297–1307 (2007).
31. P. R. Sanberg, M. D. Bunsey, M. Giordano, and A. B. Norman. The catalepsy test: ist ups and downs. *Behav. Neurosci.* **102**:748–759 (1988).
32. K. Jores, W. Mehnert, M. Drechsler, H. Bunjes, C. Johann, and K. Maeder. Investigations on the structure of solid lipid nanoparticles (SLN) and oil-loaded solid lipid nanoparticles by photon correlation spectroscopy, field-flow fractionation and transmission electron microscopy. *J. Control. Release* **95**:217–227 (2004).
33. J. C. Olivier, L. Fenart, R. Chauvet, C. Pariat, R. Cecchelli, and W. Couet. Indirect evidence that drug brain targeting using polysorbate 80-coated polybutylcyanoacrylate nanoparticles is related to toxicity. *Pharm. Res.* **16**:1836–1842 (1999).
34. J. Kreuter. Nanoparticulate systems for brain delivery of drugs. *Adv. Drug Deliv. Rev.* **47**:65–81 (2001).
35. S. Ulrike, S. Petra, U. Sven, and B. A. Sabel. Nanoparticle technology for delivery of drugs across the blood–brain barrier *J. Pharm. Sci.* **87**:1305–1307 (1998).
36. R. P. Lockmana, M. O. Oyewumi, J. M. Koziara, K. E. Roder, R. J. Mumper, and D. D. Allen. Brain uptake of thiamine-coated nanoparticles. *J .Control. Release* **93**:271–282 (2003).
37. Z. R. Zhang, J. X. Wang, and J. Lu. Optimization of the preparation of 30,50-dioctanoyl-5-fluoro-20-deoxyuridine pharmacosomes using central composite design. *Acta Pharmaceutica Sinica.* **36**:461–465 (2001).
38. Y. X. Peng, Y. L. Zhuang, and G. T. Liao. Study on bone marrow targeting daunorubicin polybutylcyanoacrylate nanoparticles. *Chin. J. Pharm.* **31**:57–61 (2000).
39. S. M. Moghimi. Mechanisms regulating body distribution of nanospheres conditioned with pluronic and tetronic block co-polymers. *Adv. Drug Deliv. Rev.* **16**:183–186 (1995).
40. P. Calvo, B. Gouritin, H. Villarroya, F. Eclancher, C. Giannavola, C. Klein, J. P. Andreux, and P. Couvreur. Quantification and localization of PEGylated polycyanoacrylate nanoparticles in brain and spinal cord during experimental allergic encephalomyelitis in the rat. *Eur. J. Neurosci.* **15**:1317–1326 (2002).
41. I. Brigger, J. Morizet, G. Aubert, H. Chacun, M. J. Terrier-Lacombe, P. Couvreur, and G. Vassal. Poly(ethylene glycol)-coated hexadecylcyanoacrylate nanospheres display a combined effect for brain tumor targeting. *J. Pharmacol. Exp. Ther.* **303**:928–936 (2002).
42. J. Kreuter. Delivery of loperamide across the blood-brain barrier with Polysorbate 80-coated polybutylcyanoacrylate nanoparticles. *Pharm. Res.* **14**:325–328 (1997).
43. J. M. Koziara, P. R. Lockman, D. D. Allen, and R. J. Mumper. *In situ* blood-brain barrier transport of nanoparticles, Pharm. *Res.* **20**:1772–1778 (2003).
44. S. C. Yang, L. F. Lu, Y. Cai, J. B. Zhu, B. W. Liang, and C. Z. Yang. Body distribution in mice of intravenously injected camptothecin solid lipid nanoparticles and targeting effect on brain. *J. Control Release* **59**:299–307 (1999).
45. S. B. Tiwari and M. M. Amiji. A Review of Nanocarrier-Based CNS Delivery Systems. *Current Drug Delivery* **3**:219–232 (2006).
46. E. L. Lane, S. C. Cheetam, and P. Jenner. Does contraversive circling in the 6-OHDA-lesioned rat indicate an ability to induce motor complications as well as therapeutic effects in Parkinson's disease. *Exp. Neurol.* **197**:284–290 (2006).